The Signature Lepton + Photon + b-jet with Missing Transverse Energy and a Measurement of the $t\bar{t}\gamma$ Cross-Section

(CDF Collaboration)

(Dated: June 12, 2008)

We present a search for anomalous production of the signature ℓ+γ+b-quark+$\not\!\!E_{\rm T}$ produced in $p\bar{p}$ collisions at $\sqrt{s} = 1.96$ TeV using 1.9 fb^{-1} of data taken with the CDF detector in Run II at the Tevatron. In addition to this signature-based search, we present a search for top pair production with an additional radiated photon, $t\bar{t} + \gamma$. We find 28 $\ell\gamma\not\!\!E_{\rm T}b$ events versus an expectation of $27.9^{+3.6}_{-3.5}$ events. Additionally requiring the events to contain at least 3 jets and to have a total transverse energy of 200 GeV, we observe 16 $t\bar{t}\gamma$ candidate events versus an expectation from non-top standard model [1] (SM) sources of $6.7^{+2.3}_{-2.1}$ Assuming the difference between the observed number and the predicted non-top SM total is due to top production, we measure the $t\bar{t}\gamma$ cross-section to be 0.15 ± 0.08 pb.

PACS numbers: 13.85.Rm, 12.60.Jv, 13.85.Qk, 14.80.Ly

The unknown nature of possible new phenomena in the energy range accessible at the Tevatron is the motivation for a "signature-based" search strategy that does not focus on a single model or class of models of new physics, but presents a wide net for new phenomena [2–4]. Here we report the results of a search for anomalous production of $\ell\gamma\not\!\!E_{\rm T}b$ events using 1850 pb^{-1} of integrated luminosity from $\bar{p}p$ collisions at $\sqrt{s} = 1.96$ TeV collected using the CDF II detector [5]. The events for the searches include production of two gauge bosons, W and γ, and two third-generation quarks, top and bottom. This search is an extension of a previous search in the lepton+photon+X signature, described in detail in Ref. [6].

A search for the production of top pairs with an additional photon, $t\bar{t}\gamma$, is a natural extension of this signature-based search, in that $t\bar{t}\gamma$ is characterized by the signature of a high-$\rm P_T$ lepton, photon, b-tagged jet, and $\not\!\!E_{\rm T}$. When one in addition requires large $\rm H_T$ and 3-or-more jets radiative top-pair events dominate the SM predictions.

The CDF II detector is a cylindrically-symmetric spectrometer designed to study $\bar{p}p$ collisions at the Fermilab Tevatron. The detector has already been described in detail in the literature [5]. Here we briefly describe the detector subsystems relevant for the analysis.

Tracking systems are used to measure the momenta of charged particles and to trigger on and identify leptons with large transverse momentum [7]. A multi-layer system of silicon strip detectors [8], which identifies tracks in both the r-ϕ and r-z views [9], and the central outer tracker (COT) [10] are contained in a superconducting solenoid that generates a magnetic field of 1.4 T. The COT is a 3.1 m long open-cell drift chamber that makes up to 96 measurements along the track of each charged particle in the region $|\eta| < 1$. Sense wires are arranged in 8 alternating axial and $\pm 2^\circ$ stereo superlayers with 12 wires each. For high momentum tracks, the COT $\rm P_T$ resolution is $\sigma_{\rm P_T}/{\rm P_T^2} \simeq 0.0017\ GeV^{-1}$.

Segmented calorimeters with towers arranged in a projective geometry, each tower consisting of an electromagnetic and a hadronic compartment [11, 12], cover the central region, $|\eta| < 1$ (CEM/CHA), and the 'end plug' region, $1 < |\eta| < 3.6$ (PEM/PHA). In both the central and end plug regions, systems with finer spatial resolution are used to make profile measurements of electromagnetic showers at shower maximum [5] for electron identification (the CES and PES systems, respectively). Electrons are reconstructed in the CEM with an $\rm E_T$ resolution of $\sigma(\rm E_T)/E_T \simeq 13.5\%/\sqrt{\rm E_T/\mathit{GeV}} \oplus 2\%$ [11] and in the PEM with an $\rm E_T$ resolution of $\sigma(\rm E_T)/E_T \simeq 16.0\%/\sqrt{\rm E_T/\mathit{GeV}} \oplus 1\%$ [13]. Jets are identified using a cone in $\eta - \phi$ space of radius 0.4 as a group of electromagnetic and hadronic calorimeter towers; the jet energy resolution is approximately $\sigma \simeq 0.1 \times \rm E_T(\mathit{GeV}) + 1.0\ \mathit{GeV}$ [14].

Muons are identified using the central CMU, CMP, and CMX [15–17] muon systems, which cover the kinematic region $|\eta| < 1$. The CMU uses four layers of planar drift chambers to detect muons with $\rm P_T > 1.4\ \mathit{GeV}$ in the central region of $|\eta| < 0.6$. The CMP consists of an additional four layers of planar drift chambers located behind 0.6 m of steel outside the magnetic return yoke, and detects muons with $\rm P_T > 2.0\ \mathit{GeV}$. The CMX detects muons in the region $0.6 < |\eta| < 1.0$ with four to eight layers of drift chambers, depending on the polar angle.

The beam luminosity is measured using two sets of gas Cherenkov counters, located in the region $3.7 < |\eta| < 4.7$. The total uncertainty on the luminosity is estimated to be 5.9%, where 4.4% comes from the acceptance and operation of the luminosity monitor and 4.0% from the calculation of the inelastic $\bar{p}p$ cross-section [18].

A 3-level trigger [5] system selects events with a high transverse momentum ($\rm P_T$) [7] electron or muon in the central region, $|\eta| \lesssim 1.0$. The trigger system selects electron candidates from clusters of energy in the central electromagnetic calorimeter. Electrons are distinguished from photons by requiring a COT track pointing at the cluster. The muon trigger requires a COT track that extrapolates to a track segment ("stub") in the muon

chambers.

Inclusive $\ell\gamma$ events are selected by requiring a central γ candidate with $E_T^\gamma > 10\ GeV$ and a central e or μ with $E_T^\ell > 20\ GeV$ originating less than 60 cm along the beam-line from the detector center and passing the "tight" selection criteria listed below.

The identification of leptons and photons is essentially the same as in the Run II $\ell\gamma + X$ search [6].

A muon candidate passing the "tight" cuts must have: a) a well-measured track in the COT; b) energy deposited in the calorimeter consistent with expectations; c) a muon "stub" in both the CMU and CMP, or in the CMX, consistent with the extrapolated COT track; and d) COT timing consistent with a track from a $p\bar{p}$ collision. An electron candidate passing the "tight" selection must have: a) a high-quality track with $P_T > 0.5\ E_T$, unless $E_T > 100\ GeV$, in which case the P_T threshold is set to 20 GeV; b) a good transverse shower profile that matches the extrapolated track position; c) a lateral sharing of energy in the two calorimeter towers containing the electron shower consistent with that expected; and d) minimal leakage into the hadron calorimeter [19].

Photon candidates are required to have no track with $P_T > 1\ GeV$, and at most one track with $P_T < 1\ GeV$, pointing at the calorimeter cluster; good profiles in both transverse dimensions at shower maximum; and minimal leakage into the hadron calorimeter [19].

To reduce background from photons or leptons from the decays of hadrons produced in jets, both the photon and the lepton in each event are required to be "isolated". The E_T deposited in the calorimeter towers in a cone in $\eta - \varphi$ space [9] of radius $R = 0.4$ around the photon or lepton position is summed, and the E_T due to the photon or lepton is subtracted. The remaining E_T is required to be less than $2.0\ GeV + 0.02 \times (E_T - 20\ GeV)$ for a photon, or less than 10% of the E_T for electrons or P_T for muons. In addition, for photons the sum of the P_T of all tracks in the cone must be less than $2.0\ GeV + 0.005 \times E_T$.

Missing transverse energy $\not\!\!E_T$ is calculated from the calorimeter tower energies in the region $|\eta| < 3.6$. Corrections are then made to the $\not\!\!E_T$ for non-uniform calorimeter response [20] for jets with uncorrected $E_T > 15\ GeV$ and $\eta < 2.0$, and for muons with $P_T > 20\ GeV$.

The $\ell\gamma\not\!\!E_T b + X$ search is defined by requiring that an event contain a "tight" electron or muon with $E_T^\ell > 20\ GeV$ [7],a photon with $E_T^\gamma > 10\ GeV$, a b-tagged jet with $E_T^{\rm jet} > 15\ GeV$, and $\not\!\!E_T > 20\ GeV$. Figures 1 and 2 show some characteristic kinematic distributions for events in the $\ell\gamma\not\!\!E_T b$ sample.

A second search, for $t\bar{t}\gamma$ events, is constructed by further requiring $H_T > 200\ GeV$ [21] and number of jets in event $N_{jets} > 2$ in addition to the $\ell\gamma\not\!\!E_T b$ requirements. Figures 3 and 4 show the corresponding kinematic distributions for events in the $t\bar{t}\gamma$ sample.

The dominant SM source of $\ell\gamma\not\!\!E_T b$ events at the Tevatron is $t\bar{t}\gamma$ production and $W\gamma$+Heavy Flavour (HF), in which a W boson decays leptonically ($\ell\nu$) and a photon is radiated from an initial-state quark, the W, or a charged final-state lepton [22]. The production of $t\bar{t}$+photon with one of the W bosons decaying leptonically and the other hadronically ('semileptonic' in Tables I and II) is estimated using MADGRAPH [23], a leading-order (LO) matrix-element event generator. The

CDF Run II Preliminary, 1.9fb^{-1}

Lepton + Photon + $\not\!\!E_T$ + b Events			
SM Source	$e\gamma b\not\!\!E_T$	$\mu\gamma b\not\!\!E_T$	$(e+\mu)\gamma b\not\!\!E_T$
$t\bar{t}\gamma$ semileptonic	2.06 ± 0.38	1.52 ± 0.28	3.58 ± 0.65
$t\bar{t}\gamma$ dileptonic	1.30 ± 0.23	1.02 ± 0.18	2.32 ± 0.41
$W^\pm c\gamma$	0.75 ± 0.16	0.72 ± 0.15	1.47 ± 0.26
$W^\pm cc\gamma$	0.08 ± 0.04	0.22 ± 0.06	0.30 ± 0.08
$W^\pm bb\gamma$	0.62 ± 0.11	0.42 ± 0.08	1.04 ± 0.17
$Z(\tau\tau)\gamma$	0.13 ± 0.09	0.11 ± 0.08	0.24 ± 0.12
WZ	0.08 ± 0.04	0.01 ± 0.01	0.09 ± 0.04
$\tau \to \gamma$ fake	0.12 ± 0.01	0.10 ± 0.01	0.22 ± 0.01
Jet faking γ	4.56 ± 1.92	3.02 ± 1.19	7.58 ± 3.11
Mistags	4.11 ± 0.41	3.54 ± 0.37	7.65 ± 0.70
QCD	1.49 ± 0.77	0^{+1}_{-0}	$1.49^{+1.30}_{-0.77}$
$ee\not\!\!E_T b$, $e \to \gamma$	1.50 ± 0.28	–	1.50 ± 0.28
$\mu e\not\!\!E_T b$, $e \to \gamma$	–	0.45 ± 0.10	0.45 ± 0.10
Predicted	$16.8 \pm 2.2(tot)$	$11.1^{+1.7}_{-1.4}(tot)$	$27.9^{+3.6}_{-3.5}(tot)$
Observed	16	12	28

TABLE I: Summary for the $\ell\gamma\not\!\!E_T b$ signature-based search. Backgrounds from WW, ZZ, and single top with an additional radiated photon are found to be negligible.

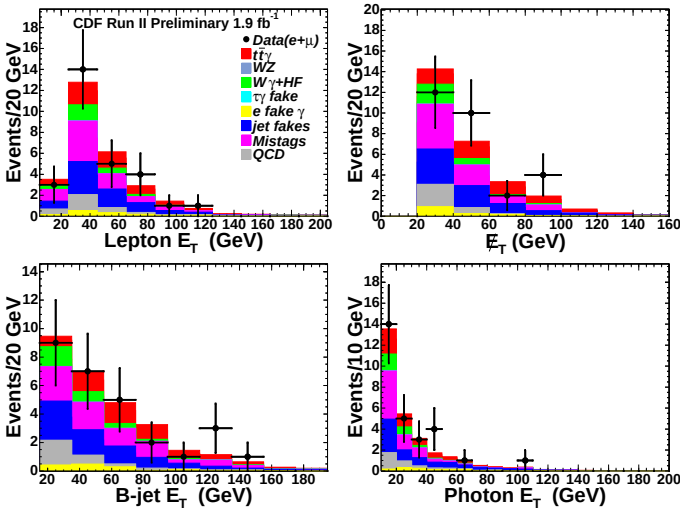

FIG. 1: The distributions for events in the $\ell\gamma\not\!\!E_T b$ sample (points) in a) the E_T of the photon; b) the E_T of the lepton; c) the missing transverse energy, $\not\!\!E_T$; and d) the E_T of the highest E_T b jet in an event. The histograms show the expected SM contributions, including estimated backgrounds from misidentified photons and leptons.

production of $t\bar{t}$+photon with both W bosons decaying leptonically (e, μ and τ channels-'dileptonic'in Tables I and II) is also estimated from the MADGRAPH MC. The SM background from a production of a W boson and a photon, accompanied by QCD production of heavy flavor quarks in the processes $Wb\bar{b}$+photon, $Wc\bar{c}$+photon, and Wc+photon, is estimated from MADGRAPH MC. Backgrounds from WW, ZZ, single top + photon are estimated to be negligible.

Initial state radiation is simulated by the PYTHIA shower Monte Carlo code [24] tuned so as to reproduce the underlying event. The generated particles are then passed through a full simulation of the detector, and these events are then reconstructed with the same reconstruction code used for the data.

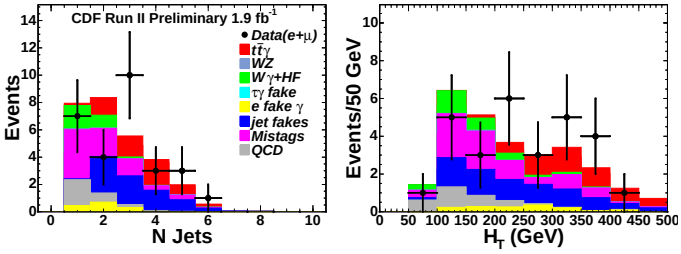

FIG. 2: The distributions for events in the $\ell\gamma\not\!\!E_{\rm T}b$ sample (points) in a) the total number of jets; b) the total transverse energy H_T, the sum of the transverse energies of the lepton, photon, jets and $\not\!\!E_{\rm T}$, for the $\ell\gamma\not\!\!E_{\rm T}b$ events. The histograms show the expected SM contributions, including estimated backgrounds from misidentified photons and leptons.

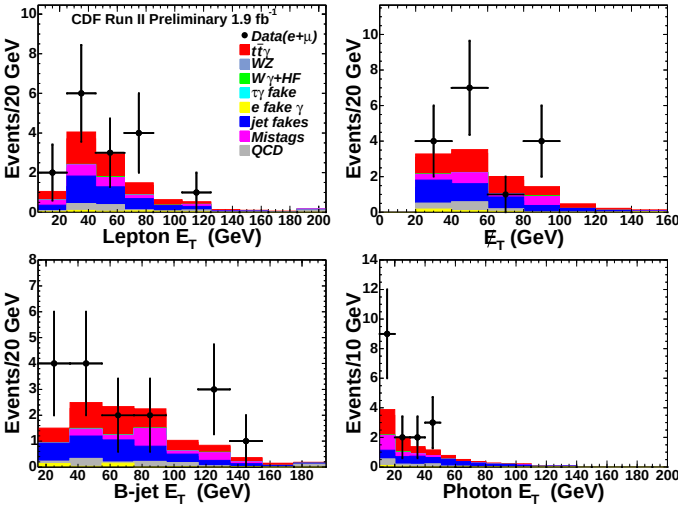

FIG. 3: The distributions for events in the $t\bar{t}\gamma$ sample (points) in a) the E_T of the photon; b) the E_T of the lepton; c) the missing transverse energy, $\not\!\!E_{\rm T}$; and d) the E_T of the highest E_T b jet in an event. The histograms show the expected SM contributions, including estimated backgrounds from misidentified photons and leptons.

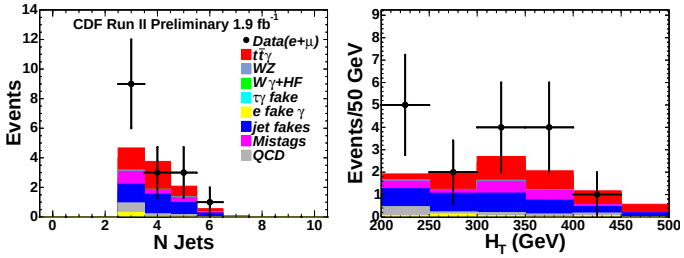

FIG. 4: The distributions for events in the $t\bar{t}\gamma$ sample (points) in a) the total number of jets; b) the total transverse energy H_T, the sum of the transverse energies of the lepton, photon, jets and $\not\!\!E_{\rm T}$, for the $\ell\gamma\not\!\!E_{\rm T}b$ events. The histograms show the expected SM contributions, including estimated backgrounds from misidentified photons and leptons.

The expected contributions from $t\bar{t}\gamma$ and $W\gamma + HF$ production to the $\ell\gamma\not\!\!E_{\rm T}b$ and $t\bar{t}\gamma$ searches are given in Tables I and II. A correction for higher-order processes (K-factor) for $t\bar{t}\gamma$ MC has been applied [25].

High P_T photons are copiously created from hadron decays in jets initiated by a scattered quark or gluon. In particular mesons such as the π^0 or η decay to photons which may satisfy the photon selection criteria. The numbers of lepton-plus-misidentified-jet events expected in the $\ell\gamma\not\!\!E_{\rm T}b$ and $t\bar{t}\gamma$ samples are determined by measuring the jet E_T spectrum in $\ell\not\!\!E_{\rm T}b$+jet and $\ell\not\!\!E_{\rm T}H_T > 200\ GeV+ > 3$ jets samples, respectively, and then multiplying by the probability of a jet being misidentified as a photon, $P_\gamma^{jet}(E_T)$, which is measured in data samples triggered on jets. The uncertainty on the number of such events is calculated by using the measured jet spectrum and the upper and lower bounds on the E_T-dependent misidentification rate.

CDF Run II Preliminary, 1.9fb^{-1}			
	$t\bar{t}\gamma$		
SM Source	$e\gamma b\not\!\!E_{\rm T}$	$\mu\gamma b\not\!\!E_{\rm T}$	$(e+\mu)\gamma b\not\!\!E_{\rm T}$
$t\bar{t}\gamma(semileptonic)$	1.97 ± 0.36	1.47 ± 0.27	3.44 ± 0.62
$t\bar{t}\gamma(dileptonic)$	0.52 ± 0.10	0.43 ± 0.08	0.95 ± 0.17
$W^{\pm}c\gamma$	$0.0^{+0.02}_{-0}$	$0.0^{+0.02}_{-0}$	$0^{+0.03}_{-0}$
$W^{\pm}cc\gamma$	$0.0^{+0.02}_{-0}$	0.01 ± 0.01	$0.01^{+0.02}_{-0.01}$
$W^{\pm}bb\gamma$	0.06 ± 0.03	0.01 ± 0.01	0.07 ± 0.03
WZ	0.02 ± 0.02	$0.0^{+0.02}_{-0}$	0.02 ± 0.02
$\tau \to \gamma$ fake	0.08 ± 0.01	0.02 ± 0.01	0.10 ± 0.01
Jet faking γ	2.37 ± 1.22	1.42 ± 0.70	3.79 ± 1.92
B-jet mistags	0.78 ± 0.20	0.83 ± 0.22	1.61 ± 0.31
QCD	0.53 ± 0.46	0^{+1}_{-0}	$0.53^{+1.10}_{-0.46}$
$ee\not\!\!E_{\rm T}b$, $e\to\gamma$	0.34 ± 0.11	–	0.34 ± 0.11
$\mu e\not\!\!E_{\rm T}b$, $e\to\gamma$	–	0.20 ± 0.06	0.20 ± 0.06
Predicted	$6.7 \pm 1.4(tot)$	$4.4^{+1.3}_{-0.8}(tot)$	$11.1^{+2.3}_{-2.1}(tot)$
Observed	8	8	16

TABLE II: Summary of the expected SM contributions to the $t\bar{t}\gamma$ search. Backgrounds from WW, ZZ, single top with an additional radiated photon are found to be negligible

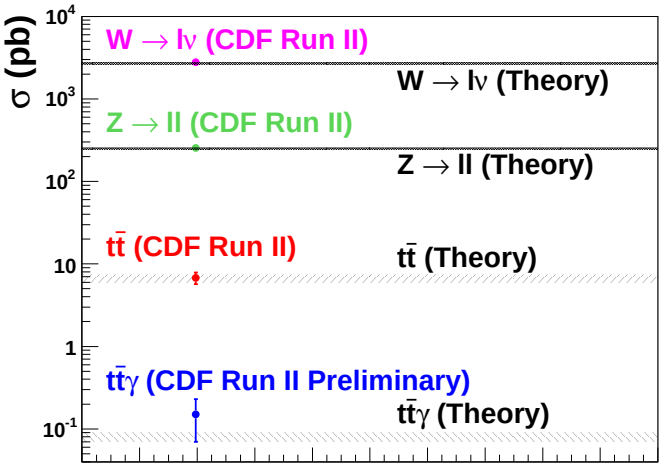

FIG. 5: The measured $\sigma_{t\bar{t}\gamma}$ compared with SM expectations and other SM cross-sections $\sigma_{W^{\pm}\to\ell^{\pm}\nu}$, $\sigma_{Z^0\to\ell^+\ell^-}$ and $\sigma_{t\bar{t}}$.

The number of "electron faking photon" events expected in the $\ell\gamma\not\!\!E_{\rm T}b$ signature is determined by measuring the photon $E_{\rm T}$ spectrum in $\ell e\not\!\!E_{\rm T}b$ samples, and then multiplying by the probability of an electron being misidentified as a photon, $P_{e\to\gamma}$, which is measured in $Z^0 \to e^+e^-$ events in which one of the electrons radiates a high-$E_{\rm T}$ photon.

To estimate the size of the mistag background, each jet in the $\ell\gamma\not\!\!E_{\rm T}$+pretagged jet sample is weighted by its mistag rate. The mistag rate per jet is measured using a large inclusive-jet data sample.

We have estimated the background due to events with jets misidentified as $\ell\gamma\not\!\!E_{\rm T}b$ signature by studying the total $P_{\rm T}$ of tracks in a cone in $\eta-\varphi$ space of radius R=0.4 around the lepton track (track isolation). We compared distribution of track isolation in our signal sample to that of the $Z^0 \to e^+e^-$ and $Z^0 \to \mu^+\mu^-$ samples (for the electron and the muon channels, respectively) and to that of the QCD background sample (generic jet sample, dominated by light-flavor jets).

The background from tau leptons faking photons is estimated from the $t\bar{t}$ PYTHIA [24] sample by selecting $\tau \to$ *hadrons* $\to \gamma$ events using MC information and then applying the same analysis cuts as for data.

We find 28 $\ell\gamma\not\!\!E_{\rm T}b$ events versus an expectation of $27.9^{+3.6}_{-3.5}$ events. We observe 16 $t\bar{t}\gamma$ candidate events versus an expectation of $11.1^{+2.3}_{-2.1}$ events. There is no significant excess in either signature.

The detection efficiency and acceptance for $t\bar{t}\gamma$ events are calculated using the MADGRAPH event generator to generate $t\bar{t}\gamma$ events with one leptonic W decay. The uncertainty on the cross-section is dominated by the statistical uncertainties associated with the small number of events observed.

The probability that the backgrounds alone (i.e. if one assumes that there is no standard model production of the $t\bar{t}\gamma$ final state) will produce 16 or more events, is 1% (2.3 σ). Assuming that the difference between the non-top background estimate and the number of observed events is due to $t\bar{t}\gamma$ SM production, we estimate the $t\bar{t}\gamma$ cross-section to be $0.15 \pm 0.08pb$. An estimate of the expected SM cross-section $\sigma_{semileptonic\ t\bar{t}\gamma} = 0.080 \pm 0.011\ pb$ is obtained from the LO MADGRAPH cross-section $\sigma_{semileptonic\ t\bar{t}\gamma} = 0.073\ pb$ multiplied by $k_{factor} = \sigma_{NLO}/\sigma_{LO} = 1.10 \pm 0.15$ [25]. An event display of a $t\bar{t}\gamma$ candidate event is shown in Figure 5.

The predicted and observed totals for both the $\ell\gamma\not\!\!E_{\rm T}b$ and $t\bar{t}\gamma$ searches are shown in Tables I and II. The predicted and observed kinematic distributions are compared in Figures 1 and 2 for the $\ell\gamma\not\!\!E_{\rm T}b$ signature, and Figures 3 and 4 for the $t\bar{t}\gamma$ search.

In conclusion, we have performed the search for inclusive lepton + photon + $\not\!\!E_{\rm T}$ + b-quark production. In addition to this signature-based search, we have performed a search for $t\bar{t}\gamma$, which is the dominant standard model process that produces this signature with large total energy ($H_{\rm T}$). We find that the numbers of events agree with SM predictions. Assuming standard model top production, the measurement of the $t\bar{t}\gamma$ cross-section $\sigma_{t\bar{t}\gamma} = 0.15 \pm 0.08pb$.

We thank the Fermilab staff and the technical staffs of the participating institutions for their vital contributions. Uli Baur, Frank Petriello, Alexander Belyaev, Edward Boos, Lev Dudko, Tim Stelzer, and Stephen Mrenna were extraordinarily helpful with the SM predictions. This work was supported by the U.S. Department of Energy and National Science Foundation; the Italian

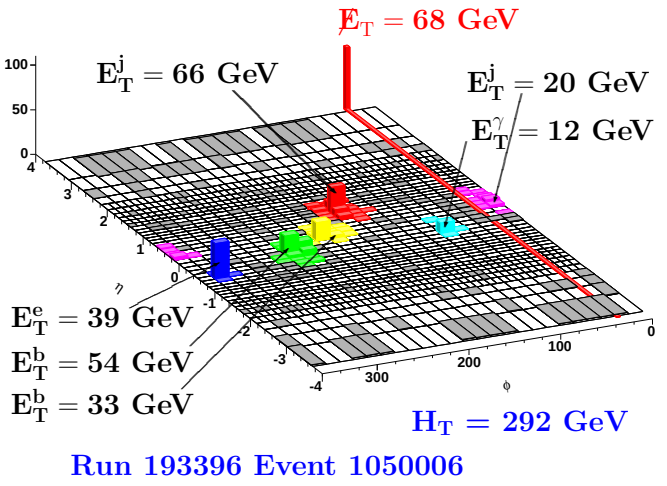

FIG. 6: The 'Lego' plot of a $t\bar{t}\gamma$ candidate event, in which the energies deposited in the calorimeter towers are displayed in the η-ϕ plane. The reconstructed top mass without the photon is 167 GeV; the photon $E_{\rm T}$ is 12 GeV.

Istituto Nazionale di Fisica Nucleare; the Ministry of Education, Culture, Sports, Science and Technology of Japan; the Natural Sciences and Engineering Research Council of Canada; the National Science Council of the Republic of China; the Swiss National Science Foundation; the A.P. Sloan Foundation; the Bundesministerium für Bildung und Forschung, Germany; the Korean Science and Engineering Foundation and the Korean Research Foundation; the Particle Physics and Astronomy Research Council and the Royal Society, UK; the Russian Foundation for Basic Research; the Comisión Interministerial de Ciencia y Tecnología, Spain; in part by the European Community's Human Potential Programme under contract HPRN-CT-2002-00292; and the Academy of Finland.

[1] S.L. Glashow, Nucl. Phys. **22** 588, (1961); S. Weinberg, Phys. Rev. Lett. **19** 1264, (1967); A. Salam, Proc. 8th Nobel Symposium, Stockholm, (1979).

[2] F. Abe *et al.* (CDF Collaboration), Phys. Rev. D **59**, 092002 (1999); F. Abe *et al.* (CDF Collaboration), Phys. Rev. Lett. **81**, 1791 (1998); D. Toback, Ph.D. thesis, University of Chicago, 1997.

[3] D. Acosta *et al.* (CDF Collaboration), Phys. Rev. D **66**, 012004 (2002); hep-ex/0110015; D. Acosta *et al.* (CDF Collaboration), Phys. Rev. Lett. **89**, 041802 (2002); hep-ex/0202004; J. Berryhill, Ph.D. thesis, University of Chicago, 2000.

[4] T. Aaltonen *et al.* [CDF Collaboration], "Model-Independent and Quasi-Model-Independent Search for New Physics at CDF,". Submitted to Phys. Rev. D; Dec. 2007, arXiv:0712.1311 [hep-ex]; T. Aaltonen *et al.* [CDF Collaboration], "Model-Independent Global Search for New High-pT Physics at CDF," Submitted to Phys.Rev.Lett; Dec. 2007, arXiv:0712.2534 [hep-ex],

[5] D. Acosta *et al.* (CDF Collaboration), Phys. Rev. D **71**, 032001 (2005).

[6] A. Abulencia *et al.* (CDF Collaboration), Phys. Rev. Lett. **97**, 031801 (2006); A. Abulencia *et al.* (CDF Collaboration), Phys. Rev. D **75**, 112001 (2007) A. Loginov, Ph.D thesis, Institute for Theoretical and Experimental Physics, Moscow, Russia, 2006.

[7] Transverse momentum and energy are defined as $\mathrm{P_T} = p\sin\theta$ and $\mathrm{E_T} = E\sin\theta$, respectively. Missing $\mathrm{E_T}$ ($\vec{\not\!\!E}_T$) is defined by $\vec{\not\!\!E}_T = -\sum_i E_T^i \hat{n}_i$, where i is the calorimeter tower number for $|\eta| < 3.6$ (see Ref. [9]), and $\hat{n}_i$ is a unit vector perpendicular to the beam axis and pointing at the i^{th} tower. We correct $\vec{\not\!\!E}_T$ for jets and muons. We define the magnitude $\not\!\!E_{\mathrm{T}} = |\vec{\not\!\!E}_T|$. We use the convention that "momentum" refers to pc and "mass" to mc^2.

[8] A. Sill *et al.*, Nucl. Instrum. Methods A **447**, 1 (2000); A. Affolder *et al.*, Nucl. Instrum. Methods A **453**, 84 (2000); C.S. Hill, Nucl. Instrum. Methods A **530**, 1 (2000).

[9] The CDF coordinate system of r, φ, and z is cylindrical, with the z-axis along the proton beam. The pseudorapidity is $\eta = -\ln(\tan(\theta/2))$.

[10] A. Affolder *et al.*, Nucl. Instrum. Methods A **526**, 249 (2004).

[11] L. Balka *et al.*, Nucl. Instrum. Methods A **267**, 272 (1988).

[12] S. Kuhlmann *et al.*, Nucl. Instrum. Methods A **518**, 39, 2004.

[13] M. G. Albrow *et al.* [CDF Collaboration], Nucl. Instrum. Meth. A **480**, 524 (2002).

[14] F. Abe *et al.*, Phys. Rev. Lett. **68**, 1104 (1992).

[15] The CMU system consists of gas proportional chambers in the region $|\eta| < 0.6$; the CMP system consists of chambers after an additional meter of steel, also for $|\eta| < 0.6$. The CMX chambers cover $0.6 < |\eta| < 1.0$.

[16] G. Ascoli *et al.* (CDF Collaboration), Nucl. Instrum. Methods A **268**, 33 (1988).

[17] T. Dorigo *et al.* (CDF Collaboration), Nucl. Instrum. Methods A **461**, 560 (2001).

[18] D. Acosta *et al.* (CDF Collaboration), Nucl. Instrum. Methods A **494**, 57 (2002).

[19] The fraction of electromagnetic energy allowed to leak into the hadron compartment $\mathrm{E_{had}/E_{em}}$ must be less than $0.055 + 0.00045 \times \mathrm{E_{em}(GeV)}$ for central electrons, less than 0.05 for electrons in the end-plug calorimeters, less than max[0.125, $0.055 + 0.00045 \times \mathrm{E_{em}\,(GeV)}$] for photons.

[20] A. Bhatti *et al.*, submitted to Nucl. Instrum. Methods, Oct. 2005; hep-ex/0510047.

[21] A. Abulencia *et al.* (CDF Collaboration), submitted to PRD; hep-ex/0602008.

[22] D. Acosta *et al.* (CDF Collaboration), Phys. Rev. Lett. **94**, 041803 (2005).

[23] T. Stelzer and W. F. Long, Comput. Phys. Commun. **81**, 357 (1994); F. Maltoni and T. Stelzer, JHEP **302**, 27 (2003).

[24] T. Sjostrand, Comput. Phys. Commun. **82** (1994) 74; S. Mrenna, Comput. Phys. Commun. **101** (1997) 232.

[25] F. Petriello, U. Baur, private communication